

(A New Proposal to Jefferson Lab PAC-27)

# $\vec{e}-^2\text{H}$ Parity Violating Deep Inelastic Scattering at CEBAF 6 GeV

December 6, 2004

(the Hall A Collaboration)

J. Arrington, K. Hafidi, R.J. Holt, D. Potterveld, P.E. Reimer (co-spokesperson), X. Zheng<sup>1</sup> (co-spokesperson)  
*Argonne National Laboratory, Argonne, IL 60439*

D. J. Margaziotis  
*California State University, Los Angeles, CA 90032*

P. Markowitz  
*Florida International University, Miami, FL 33199*

A. Afanasev, P.E. Bosted, J.-P. Chen, A. Deur, R. Feuerbach, J.-O. Hansen, D.J. Mack, R. Michaels, B. Reitz  
*Jefferson Lab, Newport News, VA 23606*

W. Korsch  
*University of Kentucky, Lexington, KY 40506*

S. Širca  
*University of Ljubljana, Slovenia*

W. Bertozzi, A.J. Puckett, O. Gayou, S. Gilad, P. Monaghan, Y. Qiang, X. Zhan  
*Massachusetts Institute of Technology, Cambridge, MA 02139*

J.R. Calarco  
*University of New Hampshire, Durham, NH 03824*

E.J. Beise  
*University of Maryland, College Park, MD 20742*

K. Kumar, K. Paschke  
*University of Massachusetts Amherst, Amherst, MA 01003*

J. Erler  
*Universidad Nacional Autónoma de México, 01000 México D. F., México*

R. Gilman, C. Glashausser, X. Jiang, R. Ransome  
*Rutgers, The State University of New Jersey, Piscataway, NJ 08855*

P. Decowski  
*Smith College, Northampton, MA 01063*

P. Souder, R. Holmes  
*Syracuse University, Syracuse, NY 13244*

G.D. Cates, N. Liyanage, V. Nelyubin, J. Singh, R. Snyder, W.A. Tobias  
*University of Virginia, Charlottesville, VA 22904*

---

<sup>1</sup>Email: xiaochao@jlab.org

## Abstract

We propose to measure the parity violating (PV) asymmetry  $A_d$  in  $\vec{e}-^2\text{H}$  deep inelastic scattering (DIS) at  $Q^2 = 1.10$  and  $1.90 \text{ (GeV/c)}^2$  at  $x \approx 0.3$ . The measurements will constrain the poorly known effective coupling constant combination  $(2C_{2u} - C_{2d})$ . Assuming the Standard Model values of  $(2C_{1u} - C_{1d})$ , (tested separately by combining the Cs atomic parity violation (APV) experiments and the future Qweak experiment), the expected uncertainty is  $\Delta(2C_{2u} - C_{2d}) = \pm 0.03$ , a factor of eight improvement. The measurement also allows the extraction of couplings  $C_{3q}$  from high energy  $\mu\text{-C}$  DIS data. Precision measurements of all phenomenological couplings are essential to comprehensively search for possible physics beyond the Standard Model.

Comparison of the two measurements ( $Q^2 = 1.10 \text{ (GeV/c)}^2$  and  $Q^2 = 1.90 \text{ (GeV/c)}^2$ ) will provide the first significant constraint on higher-twist (HT) effects in PV DIS, at the level of  $2.7\%/Q^2$ . It will provide an important guide on the future DIS-parity program with the 12 GeV upgrade, for which the ultimate goal is to extract  $\sin^2 \theta_W$  from the asymmetry free from hadronic effects. This could also have immediate impact on other DIS analyzes, such as the extraction of  $\sin^2 \theta_W$  from  $\nu - N$  DIS (NuTeV) and the extraction of the strong coupling constant  $\alpha_s$  from DIS data at low  $Q^2$ .

We plan to use a 25-cm liquid deuterium target in Hall A and a  $85\text{-}\mu\text{A}$  6.0-GeV beam with 80% polarization. An upgrade is needed for the Compton polarimeter and a fast counting data acquisition system will be developed for the proposed measurement. These enhancements to the experimental capabilities will be essential for future parity-violation experiments at JLab. The total beam time request is for 46 days, consisting of two phases: 13 days for phase I and 33 days for phase II.

## Contents

<b>1</b>	<b>Motivation</b>	<b>4</b>
1.1	Phenomenological WNC Couplings at Low $Q^2$	4
1.2	The Running of $\sin^2 \theta_W$ and The NuTeV Anomaly	6
1.3	Parity Violating Deep Inelastic Scattering (DIS-parity)	7
1.4	Formalism for $\vec{e}-^2\text{H}$ Parity Violating DIS	8
1.5	Higher-Twist Effects	9
1.6	Exploring Physics Beyond the Standard Model	11
1.6.1	DIS-Parity and New Physics	11
1.6.2	$Z'$ Searches	12
1.6.3	Compositeness and Leptoquark (LQ)	12
<b>2</b>	<b>Experimental Setup</b>	<b>13</b>
2.1	Overview	13
2.2	Beam Line	14

2.3	Parity DAQ (Hall A) . . . . .	14
2.4	The Liquid Deuterium Target . . . . .	15
2.4.1	Boiling Effect . . . . .	15
2.4.2	Helicity Dependent Density Fluctuation . . . . .	15
2.5	Luminosity Monitor . . . . .	15
2.6	Spectrometers . . . . .	16
2.7	Fast Counting DAQ . . . . .	16
2.8	Data Analysis . . . . .	18
2.8.1	Extracting Asymmetry $A_d$ from Data . . . . .	18
2.8.2	Extracting $2C_{2u} - C_{2d}$ from $A_d$ . . . . .	18
<b>3</b>	<b>Expected Uncertainties and Rate Estimation</b>	<b>19</b>
3.1	Deadtime Correction . . . . .	19
3.2	Target Purity, Density Fluctuation and Other False Asymmetries . . . . .	19
3.3	Target End Cap Contamination . . . . .	19
3.4	Pion Background . . . . .	20
3.5	Pair Production Background . . . . .	21
3.6	Electromagnetic (EM) Radiative Correction . . . . .	21
3.7	Electroweak Radiative Correction . . . . .	22
3.8	Experimental Uncertainties ( $Q^2$ and the acceptance) . . . . .	22
3.9	Parton Distribution Functions and Ratio $R$ . . . . .	22
3.10	Charge Symmetry Violation (CSV) . . . . .	23
3.11	Rate Estimation and Kinematics Optimization . . . . .	24
3.12	Error Budget . . . . .	26
<b>4</b>	<b>Beam Time Request</b>	<b>26</b>
4.1	Beam Time Request . . . . .	26
4.2	Beam Time Allocation for Running in Two Phases . . . . .	27
4.3	Overview of Instrumentation and Cost Estimate . . . . .	28
<b>5</b>	<b>Summary</b>	<b>28</b>

# 1 Motivation

## 1.1 Phenomenological WNC Couplings at Low $Q^2$

An important way to test the Standard Model (SM) is to measure weak neutral current (WNC) interactions at  $Q^2 \ll M_Z^2$ . Pseudoscalar observables can be constructed from a product of vector- and axial-vector couplings. In electron-quark scattering with two active quark flavors, there are 6 possible phenomenological couplings  $C_{1,2,3u(d)}$ . In the SM, there are definite predictions for these couplings in terms of the weak mixing angle  $\theta_W$ . Any deviation from the SM could indicate possible new physics, and that the SM could be a piece of some larger framework [1]. We will briefly describe some possible new physics scenarios in section 1.6.

We will summarize  $\theta_W$  measurements at  $Q^2 \ll M_Z^2$  in the next section. Here we will focus on  $C_{iq}$  as they are relevant to the main goal of the proposed measurements. Coefficients  $C_{iq}$  are products of weak charges given at tree level by

$$C_{1u} = g_A^e g_V^u = -\frac{1}{2} + \frac{4}{3} \sin^2(\theta_W), \quad (1)$$

$$C_{1d} = g_A^e g_V^d = \frac{1}{2} - \frac{2}{3} \sin^2(\theta_W), \quad (2)$$

$$C_{2u} = g_V^e g_A^u = -\frac{1}{2} + 2 \sin^2(\theta_W), \quad (3)$$

$$C_{2d} = g_V^e g_A^d = \frac{1}{2} - 2 \sin^2(\theta_W), \quad (4)$$

$$C_{3u} = g_A^e g_A^u = -1/2 \quad \text{and} \quad (5)$$

$$C_{3d} = g_A^e g_A^d = +1/2. \quad (6)$$

$C_{1u(d)}$  represents the axial  $Z$ -electron coupling  $g_A^e$  times the vector  $Z$ - $u(d)$  quark coupling  $g_V^{u(d)}$ , and the  $C_{2u(d)}$  is the vector  $Z$ -electron coupling  $g_V^e$  times the axial  $Z$ - $u(d)$  quark coupling  $g_A^{u(d)}$ . Similarly, the  $C_{3q}$  are the products of axial-vector electron and quark couplings, and are therefore  $C$ -violating and parity conserving. Each of the  $C_{iq}$  terms might be sensitive to physics beyond the SM in different ways.

Among experiments (finished or planned) which will test the Standard Model and the search for new physics, some are purely leptonic (E158) and are not sensitive to new interactions involving quarks, some are semi-leptonic (APV, Qweak) but can only access the weak couplings  $C_{1q}$ . In contrast to  $C_{1q}$ , the weak coupling  $C_{2q}$  and  $C_{3q}$  are poorly known.

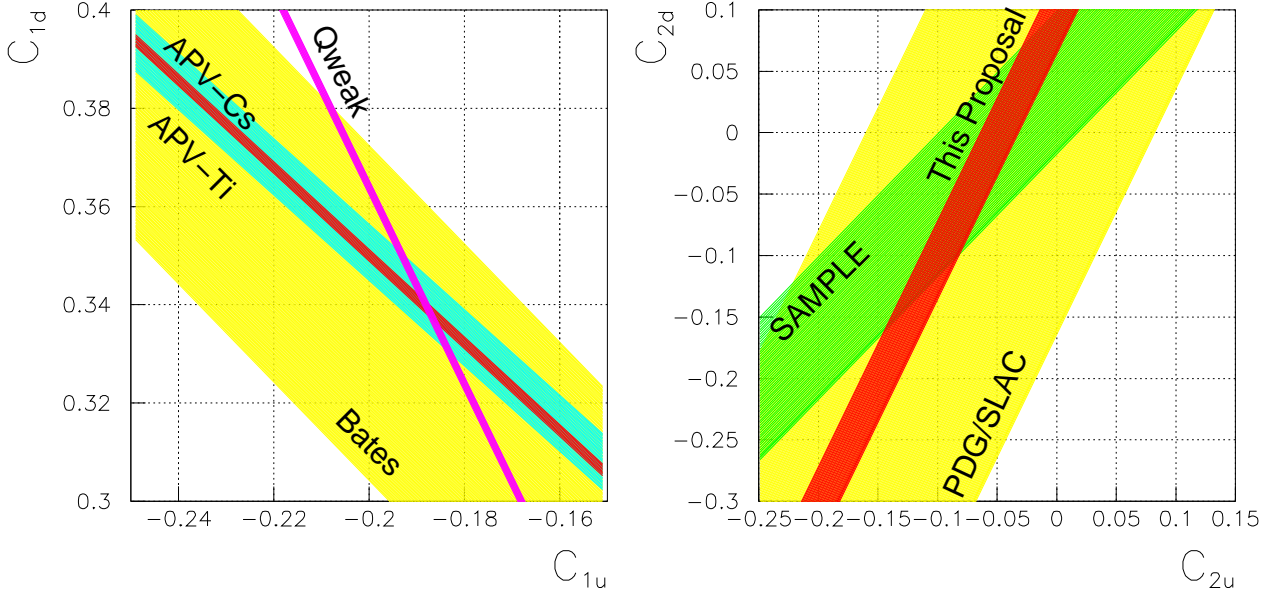
Table 1 summarizes the current knowledge of  $C_{iq}$  [2]. From existing data,  $2C_{2u} - C_{2d} = -0.08 \pm 0.24$  [3]. This constraint is poor and must be improved in order to enhance sensitivity to many possible extensions of the SM, such as quark compositeness and new gauge bosons.  $e^-^2\text{H}$  PV DIS can provide precise data on  $2C_{2u} - C_{2d}$  which are not accessible through other processes. We expect to improve the uncertainty on  $2C_{2u} - C_{2d}$  by a factor of eight.

The eD DIS experiment proposed here will also impact our knowledge of the  $C_{3q}$ . The only available measurement sensitive to these is the CERN  $\mu^\pm\text{C}$  DIS experiment [6] (see Table 1). The combination  $2C_{3u} - C_{3d}$  is only known to about 50% precision, which is partly due to a large global correlation coefficient of 0.82 with the  $C_{1q}$  and  $C_{2q}$ . The experiment proposed here would reduce this correlation to  $< 6\%$ , essentially decoupling the CERN combination,  $2C_{3u} - C_{3d}$ , and reducing its uncertainty by more than 40%.

Table 1: Existing data on  $P$  or  $C$  violating coefficients  $C_{iq}$  from Ref. [2]. The uncertainties are combined (in quadrature) statistical, systematic and theoretical uncertainties. The Bates  $e^-D$  quasi-elastic (QE) results on  $C_{2u} - C_{2d}$  are from Ref. [4]. For some of the quantities listed here, global analysis gives slightly different values, please see Ref. [5] for the most recent updates.

facility	process	$\langle Q^2 \rangle$ (GeV/c) $^2$	$C_{iq}$ combination	result	SM value
SLAC	$e^-D$ DIS	1.39	$2C_{1u} - C_{1d}$	$-0.90 \pm 0.17$	$-0.7185$
SLAC	$e^-D$ DIS	1.39	$2C_{2u} - C_{2d}$	$+0.62 \pm 0.81$	$-0.0983$
CERN	$\mu^\pm C$ DIS	34	$0.66(2C_{2u} - C_{2d})$ $+ 2C_{3u} - C_{3d}$	$+1.80 \pm 0.83$	$+1.4351$
CERN	$\mu^\pm C$ DIS	66	$0.81(2C_{2u} - C_{2d})$ $+ 2C_{3u} - C_{3d}$	$+1.53 \pm 0.45$	$+1.4204$
Mainz	$e^-Be$ QE	0.20	$2.68C_{1u} - 0.64C_{1d}$ $+ 2.16C_{2u} - 2.00C_{2d}$	$-0.94 \pm 0.21$	$-0.8544$
Bates	$e^-C$ elastic	0.0225	$C_{1u} + C_{1d}$	$0.138 \pm 0.034$	$+0.1528$
Bates	$e^-D$ QE	0.1	$C_{2u} - C_{2d}$	$-0.042 \pm 0.057$	$-0.0624$
Bates	$e^-D$ QE	0.04	$C_{2u} - C_{2d}$	$-0.12 \pm 0.074$	$-0.0624$
JLAB	$e^-p$ elastic	0.03	$2C_{1u} + C_{1d}$	approved	$+0.0357$
--	$^{133}Cs$ APV	0	$-376C_{1u} - 422C_{1d}$	$-72.69 \pm 0.48$	$-73.16$
--	$^{205}Tl$ APV	0	$-572C_{1u} - 658C_{1d}$	$-116.6 \pm 3.7$	$-116.8$

Figure 1: The effective couplings  $C_{1u}, C_{1d}$  (left),  $C_{2u}$  and  $C_{2d}$  (right). The future Qweak experiment (purple band), combined with the APV-Cs result (red band), will provide the most precise data and the best Standard Model test on  $C_{1u}$  and  $C_{1d}$ . The SAMPLE result for  $C_{2u} - C_{2d}$  at  $Q^2 = 0.1$  (GeV/c) $^2$  is shown. Assuming the SM prediction of  $2C_{1u} - C_{1d}$ , the value of  $2C_{2u} - C_{2d}$  can be determined from the proposed measurement to  $\Delta(2C_{2u} - C_{2d}) = 0.03$  (red band).

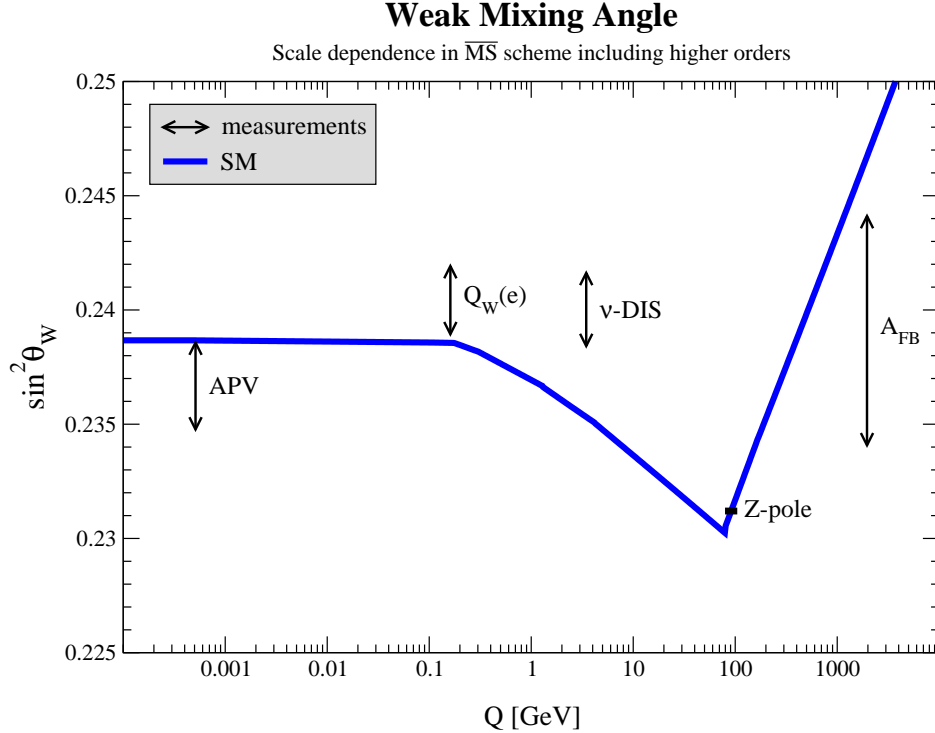


## 1.2 The Running of $\sin^2 \theta_W$ and The NuTeV Anomaly

The weak mixing angle,  $\theta_W$ , is one of the fundamental parameters of the Standard Model. Electroweak radiative corrections induce a variation of the effective value of  $\sin^2(\theta_W)$  with momentum transfer  $Q^2$ , with a minimum near the  $Z$ -pole  $Q^2 = M_Z^2$ . This variation, referred to as the “running of  $\sin^2 \theta_W$ ”, can be calculated within the Standard Model (SM) framework [7]. Testing this prediction requires a set of precision measurements at  $Q^2 \ll M_Z^2$  with sufficiently small and well understood theoretical and experimental uncertainties associated with the extraction of  $\sin^2 \theta_W$ , such that one can interpret the results with confidence.

At the  $Z$ -pole, the value of  $\sin^2(\theta_W)$  has been well established from a number of measurements [14, 15]. Combined with measurements of the  $W$  and  $t$  quark masses from the Tevatron, the average of all existing measurements gives the remarkably precise value  $\sin^2 \theta_W(M_Z)_{\overline{MS}} = 0.23120 \pm 0.00015$  [5] in the Modified Minimal Subtraction ( $\overline{MS}$ ) scheme. However, careful comparison of measurements involving lepton and hadron electroweak couplings at the  $Z$ -pole has recently revealed a three standard deviation inconsistency, which strongly hints at physics beyond the Standard Model or a significant systematic error underestimate in one or more exper-

Figure 2: The running of  $\sin^2 \theta_W$  shown as a function of  $Q^2$  [8]. Shown are the existing Atomic Parity Violation (APV) cesium measurement [9], the existing neutrino DIS (NuTeV) [10] measurements and  $Z \rightarrow \bar{b}b$  decay asymmetry measurement ( $Z$ -pole) [11], along with expected uncertainty of the approved JLAB  $Q_{\text{weak}}$  [12] and the recently completed SLAC Møller (E158) [13] experiments.



iments [11].

Away from the  $Z$ -pole, there exist three precision measurements<sup>2</sup>. The first measurement is the atomic parity violation (APV) on the cesium (Cs). While an earlier analysis claimed a two standard deviation from the SM prediction [17], the atomic theory corrections associated with the extraction of  $\sin^2 \theta_W$  from Cs APV have changed significantly, changing the result to be in reasonably good agreement with the SM [9].

The second measurement away from the  $Z$ -pole was performed by the NuTeV collaboration [10]. The value of  $\sin^2 \theta_W$  extracted from the ratios of neutral current to charged current  $\nu$  and  $\bar{\nu}$  DIS cross sections on an iron target at  $Q^2 \approx 20 \text{ (GeV/c)}^2$  is found to be  $3\sigma$  above the SM prediction. The NuTeV result triggered significant theoretical interest. However, before all possible hadronic effects are excluded, it is too early to say that this result indicates the existence of physics beyond the SM. Possible hadronic effects include charge symmetry violation (CSV) [18], higher-twist effects, nuclear effects of the iron target, and asymmetry in the average momentum carried by the strange sea:  $\int x[s(x) - \bar{s}(x)]dx \neq 0$ .

The third measurement is the recently completed Møller experiment (E158) at SLAC [13]. The value of  $\sin^2 \theta_W$  was extracted from the asymmetry  $A_{LR}$  of Møller scattering at  $Q^2 = 0.026 \text{ (GeV/c)}^2$ . Their preliminary result is about one standard deviation above the SM value [19]. In addition to APV, NuTeV and E158, the Qweak experiment planned at JLAB Hall C will measure  $\sin^2 \theta_W$  at  $Q^2 \approx 0.03 \text{ (GeV/c)}^2$  using  $\vec{e} - p$  elastic scattering.

### 1.3 Parity Violating Deep Inelastic Scattering (DIS-parity)

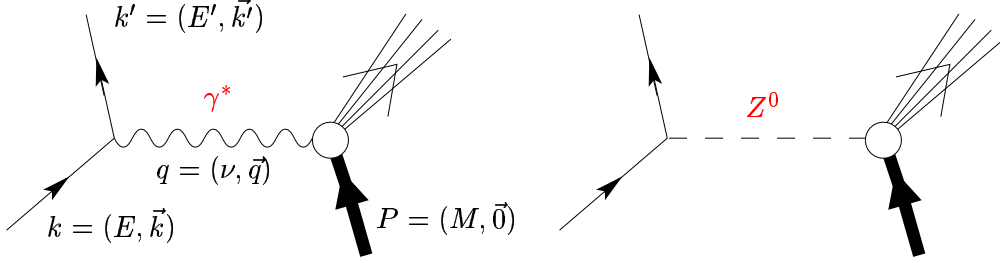
Historically, the observation of a parity violating asymmetry in DIS played a key role in establishing the validity of the Standard Model. In the 1970's, DIS-Parity at SLAC confirmed the SM prediction for the structure of weak neutral current interactions [20]. These results were consistent with a  $\sin^2 \theta_W \approx 1/4$ , implying a tiny  $V(\text{electron}) \times A(\text{quark})$  neutral current interaction. Subsequent measurements performed at both very low energy scales (APV) as well as at the  $Z$ -pole have been remarkably consistent with the results of this early DIS-parity measurement. We now briefly review the principle of the PV mechanism for  $e - N$  DIS. The detailed formalism for  $\vec{e} - {}^2\text{H}$  PV DIS will be given in the next section.

We consider electron scattering on a fixed nuclear target. We denote by  $m$  the electron mass,  $k = (E, \vec{k})$  and  $k' = (E', \vec{k}')$  the initial and final electron four-momenta; the target has a mass  $M_T$  and its initial four-momentum is  $P = (E_t, \vec{P})$ ; the final state of the target is not detected. For a fixed target, one has  $P = (M_T, \vec{0})$  in the laboratory frame. Electrons can scatter off a nuclear target by exchanging either a virtual photon ( $\gamma^*$ ) or a virtual  $Z^0$ , as shown in Fig. 3. Until 1977, electrons had been used solely as an electromagnetic probe of the nucleon because the amplitude of weak neutral-current scattering at low energy is small. A number of facilities (JLAB, SLAC, MIT-Bates, Mainz) now can provide high enough luminosity to make feasible studies of the nucleon *via* its weak neutral current coupling. The weak neutral current can be accessed by measuring a parity-violating asymmetry that is proportional to the interference term between weak and electromagnetic scattering amplitudes [21].

---

<sup>2</sup>Also note that the latest analysis on the muon  $g - 2$  gives a  $1.9\sigma$  deviation from the SM value, see p. 119 of Ref. [16].

Figure 3: Tree-level Feynman diagrams for electron scattering.



The scattering amplitude for the process is a product of currents for the electron and the hadron, sandwiched around the photon and the  $Z^0$  propagator  $\mathcal{M}_\gamma$  and  $\mathcal{M}_Z$ :

$$\mathcal{M}_\gamma = j_\mu \left( \frac{1}{q^2} \right) J^\mu ; \quad \mathcal{M}_Z = j_\mu \left( \frac{1}{M_Z^2} \right) J^\mu . \quad (7)$$

We consider a longitudinally polarized electron beam. For the weak amplitude, we use  $\mathcal{M}_Z^r$  and  $\mathcal{M}_Z^l$  for the incident right- and left-handed electrons, respectively. The cross sections for scattering right- and left-handed electrons off an unpolarized target are proportional to the square of the total amplitudes:

$$\sigma^r \propto (\mathcal{M}_\gamma + \mathcal{M}_Z^r)^2 , \quad \sigma^l \propto (\mathcal{M}_\gamma + \mathcal{M}_Z^l)^2 . \quad (8)$$

The parity-violating asymmetry can be written as

$$A_{LR} \equiv \frac{\sigma^r - \sigma^l}{\sigma^r + \sigma^l} = \frac{(\mathcal{M}_\gamma + \mathcal{M}_Z^r)^2 - (\mathcal{M}_\gamma + \mathcal{M}_Z^l)^2}{(\mathcal{M}_\gamma + \mathcal{M}_Z^r)^2 + (\mathcal{M}_\gamma + \mathcal{M}_Z^l)^2} \approx \frac{\mathcal{M}_Z^r - \mathcal{M}_Z^l}{\mathcal{M}_\gamma} . \quad (9)$$

Measuring the parity-violating asymmetry allows one to access the weak neutral current in a ratio of amplitudes rather than the square of this ratio, greatly enhancing its relative contribution. We can make an estimation of the asymmetry from the ratio of the propagators:

$$A_{LR} \approx \frac{Q^2}{M_Z^2} \approx 120 \text{ ppm at } Q^2 = 1 \text{ (GeV}/c)^2 \quad (10)$$

using  $M_Z = 91.2 \text{ GeV}$  [5].

#### 1.4 Formalism for $\vec{e} - {}^2\text{H}$ Parity Violating DIS

The parity violating asymmetry for longitudinally polarized electrons scattering off an unpolarized deuteron target is given by [21, 22]

$$\begin{aligned} A_d &\equiv \frac{\sigma^r - \sigma^l}{\sigma^r + \sigma^l} \\ &= \left( \frac{3G_F Q^2}{\pi \alpha 2\sqrt{2}} \right) \frac{2C_{1u}[1 + R_c(x)] - C_{1d}[1 + R_s(x)] + Y(2C_{2u} - C_{2d})R_v(x)}{5 + R_s(x) + 4R_c(x)} , \end{aligned} \quad (11)$$



Here, the lightest isoscaler target, deuterium, is used in order to minimize the uncertainty due to parton distribution ratio  $d(x)/u(x)$  while keeping the uncertainty due to nuclear effect small. In Eq. (11), the coefficients  $C_{1,2u(d)}$  are given by Eq. (1-4),  $G_F = 1.166 \times 10^{-5} \text{ (GeV)}^{-2}$  is the Fermi weak interaction coupling constant, and

$$Y = \frac{1 - (1 - y)^2}{1 + (1 - y)^2 - y^2 R / (1 + R)} \quad (12)$$

with  $R \equiv \sigma_L / \sigma_T$ ,  $y = \nu / E$  and  $\nu = E - E'$  the energy loss of the incident electron.

The ratios  $R_c$ ,  $R_s$  and  $R_v$  are given by the quark distribution functions:

$$\begin{aligned} R_c(x) &\equiv \frac{2(c(x) + \bar{c}(x))}{u(x) + \bar{u}(x) + d(x) + \bar{d}(x)}, \\ R_s(x) &\equiv \frac{2(s(x) + \bar{s}(x))}{u(x) + \bar{u}(x) + d(x) + \bar{d}(x)} \\ \text{and } R_v(x) &\equiv \frac{u_V(x) + d_V(x)}{u(x) + \bar{u}(x) + d(x) + \bar{d}(x)}, \end{aligned} \quad (13)$$

with  $u_V(x)$  and  $d_V(x)$  the valence quark distributions,  $u(x) = u_V(x) + u_{sea}(x) + \bar{u}(x)$ ,  $d(x) = d_V(x) + d_{sea}(x) + \bar{d}(x)$ ,  $s(x) = s_{sea}(x) + \bar{s}(x)$  and  $c(x) = c_{sea}(x) + \bar{c}(x)$ .

At high  $x$  one has  $R_c \approx 0$ ,  $R_s \approx 0$  and  $R_v \approx 1$ , thus the uncertainty in  $(2C_{2u} - C_{2d})$  due to the error in  $A_d$  is

$$\frac{\delta(2C_{2u} - C_{2d})}{(2C_{2u} - C_{2d})} \approx \frac{\delta A_d}{A_d} \left[ 1 - \frac{1}{Y} \frac{2C_{1u} - C_{1d}}{2C_{2u} - C_{2d}} \right]. \quad (14)$$

Therefore measurements at larger  $Y$  are more sensitive to  $(2C_{2u} - C_{2d})$ . This can also be seen by an inspection of Eq. (11).

## 1.5 Higher-Twist Effects

Among all hadronic effects that could contribute to PV electron scattering observables, the higher-twist (HT) effect is expected to be the most probable for kinematics at JLab. Here higher-twist effects refer to the fact that the color interactions between the quarks become stronger at low  $Q^2$  and the process cannot be described by the leading twist diagram of Fig. 3. For electromagnetic scattering processes, these interactions introduce a scaling violation to the structure functions in the low  $Q^2$  region below  $1 \text{ (GeV}/c)^2$  that is stronger than the  $\ln(Q^2)$ -dependence of the DGLAP equations of pQCD. For PV  $\vec{e}-^2\text{H}$  scattering, HT effects start from twist-four terms which diminish as  $1/Q^2$ .

The theory for HT effects is not well established. Most of the knowledge for HT is from data on DIS structure functions  $F_1$ ,  $F_2$ ,  $g_1$  and  $g_2$ . When determining the HT effects from these data, the leading twist contribution often cannot be subtracted cleanly because of the uncertainty due to the cutoff in summing the  $\alpha_s$  series, and the uncertainty in  $\alpha_s$  itself in the low  $Q^2$  region. The first parameterization of the HT coefficient  $C_{HT}$  showed sizable effect for all  $x$  values that increases dramatically at higher  $x$  [23]. In this calculation the pQCD  $Q^2$ -evolution was removed up to Next-Leading-Order (NLO). The latest fit to the HT coefficient, however, shows that the

effect for  $0.1 < x < 0.4$  diminishes quickly to  $< 1\%/Q^2$  as higher order terms (NNLO and NNNLO) are included when evaluating the leading-twist term [24].

There is almost no data on the HT contribution to PV observables. Theoretically, estimates of the twist-four corrections to the asymmetry in  $\vec{e}-^2\text{H}$  scattering have been carried out in various models. In a work by Castorina and Mulders [25], the HT contribution to the  $\vec{e}-^2\text{H}$  asymmetry was evaluated in the MIT bag model and was found to be 0.3% at  $Q^2 = 1.0 \text{ (GeV/c)}^2$ . In a similar work by Fajfer and Oakes where in addition the deuteron matrix element of the operators was used, it was found that the higher-twist effects decrease the value of  $\sin^2 \theta_W$  by less than 1% [26]. This corresponds to  $< 2\%$  contribution to the asymmetry.

The second approach to estimate HT correction to PV DIS is based on experimental data on  $C_{HT}$  and the assumption that the HT effects partly cancel in the numerator and the denominator of the asymmetry. Presumably, the higher twist dynamics is the same for the  $\gamma^*$  and  $Z_0$  exchange processes in PV DIS as that for  $F_2$ , hence cancel in the asymmetry. One possible effect that does not cancel comes from the different coupling strength of the EM and weak interactions in the interference term, which is proportional to the EM and weak charges, respectively. Quantitative calculations for the HT correction to  $A_d$  were performed in the QCD LO, NLO and NNLO framework [27]. Parameterization of  $C_{HT}$  by Virchaux and Milsztajn [23] was used as an input. The results show the HT correction to  $A_d$  is at level of  $1\%/Q^2$  for  $0.1 < x < 0.3$  in NLO or higher order analysis.

One interesting remark is that, the HT corrections to DIS-parity and to NuTeV are connected through models, such as the one given by Gluck and Reya [28]. In this reference, it was shown that although the NuTeV measurement was performed at  $\langle Q^2 \rangle = 20 \text{ (GeV/c)}^2$ , the HT contribution to the typically measured Paschos-Wolfenstein (P-W) ratio could be of the same magnitude as that to the PV DIS observable at  $Q^2 \approx 2 \text{ (GeV/c)}^2$ . Because the P-W ratio measured by NuTeV is 2.5% lower than the SM value, a 2.5% HT correction to this ratio will remove the  $3\sigma$  anomaly. Note that through model of Ref.[28], a 2.5% contribution at  $Q^2 = 2 \text{ (GeV/c)}^2$  implies the same magnitude HT contribution to our high  $Q^2$  measurement and a 5% contribution to our low  $Q^2$  measurement. Since we will measure the asymmetry to 2.08% at the low  $Q^2$  point, we will be able to observe it if the HT is indeed the dominant reason of the NuTeV anomaly. Therefore, depending on the future experimental situation and the outcome of the experiment proposed here, one will either gain a better understanding of the NuTeV discrepancy, or else rule in or out models of HT effects.

Overall, most theories predict that the HT contribution to  $A_d$  is at the  $1\%/Q^2$  level. If so, the effect at our high  $Q^2$  point will be about  $1/5$  of the statistical error and will not be significant. However, there has been no experimental proof of these theories and thus if a large deviation from the SM is observed, HT will be the most probable reason. Therefore we will measure  $A_d$  at  $Q^2 = 1.10 \text{ (GeV/c)}^2$ . If the HT contribution is statistically significant at the high  $Q^2$  measurement, it will show up at this low  $Q^2$ . This first observation of the HT effect in PV asymmetries will also provide crucial input to the future DIS-parity program at 12 GeV, and may help to explain the NuTeV anomaly.

## 1.6 Exploring Physics Beyond the Standard Model

Although there exists a large amount of data confirming the electroweak sector of the SM at a level of a few 0.1%, there also exist strong conceptual reasons (e.g., the so-called high-energy desert from  $M_{weak} \approx 250$  GeV up to the reduced Planck scale  $M_P \approx 2.4 \times 10^{18}$  GeV, and the unexplained origins of mass and violation of discrete symmetries) to believe that the SM is only a piece of some larger framework [1]. While this framework should provide answers to the conceptual puzzles of the SM, it should not spoil the successful predictions of the SM for most existing electroweak data. Phenomenologically, the observations of neutrino oscillations already provide the first discovery of a type of effect that cannot be understood in the confines of the SM. Hence there is intense interest in the search for new physics. In this section we first describe how DIS-parity can explore new physics in a somewhat different way than Qweak, E158 and NuTeV. We then give a few possible models for new physics that might be explored via measurement of  $A_d$  and  $C_{2q}$ 's for the precision proposed here, namely the search for extra neutral gauge boson  $Z'$ , compositeness and leptoquark.

### 1.6.1 DIS-Parity and New Physics

If free from nuclear and QCD higher-twist effects, the DIS-parity measurement will explore possible new physics beyond the Standard Model. DIS-parity involves exchange of  $Z^0$  between electrons and quarks and thus is sensitive to physics that might not be seen in purely leptonic observables, such as the precision  $A_{LR}$  at SLC and  $A_{FB}^l$  at LEP. There is currently a  $3\sigma$  disagreement [11] in  $\sin^2 \theta_W$  between purely leptonic and semi-leptonic observables at the  $Z$ -pole from SLC and LEP. The recent NuTeV [10] result on  $\sin^2 \theta_W$  at low  $Q^2$  involves a particular set of semi-leptonic charged and neutral current reactions and is  $3\sigma$  from the SM prediction. A precision measurement of DIS-parity will add a clean semi-leptonic observable to the world data below the  $Z$ -pole and may provide essential clues as to the source of the latter of these discrepancies.

A precision DIS-parity measurement would also examine the  $Z$  coupling to electrons and quarks at low  $Q^2$  far below the  $Z$ -pole. This is important because DIS-parity is sensitive to a particular combination of couplings and has completely different sensitivities to new physics than other semi-leptonic processes (e.g., Qweak). For example, the quark and lepton compositeness is accessible only through  $C_{2q}$  but not  $C_{1q}$  if a particular symmetry [SU(12)] is respected. DIS-parity will significantly strengthen the constraints on these possible new physics.

The mass limit to which the proposed measurement is sensitive to can be estimated using the following model independent analysis. Analogous to Eq. (25-27) of Ref. [29], the low energy effective electron-quark Lagrangian of the form  $V(e) \times A(q)$  is given by

$$\mathcal{L} = \mathcal{L}_{SM}^{PV} + \mathcal{L}_{NEW}^{PV} \quad (15)$$

where

$$\mathcal{L}_{SM}^{PV} = -\frac{G_F}{\sqrt{2}} \bar{e} \gamma_\mu e \sum_q C_{1q} \bar{q} \gamma^\mu \gamma^5 q \quad (16)$$

$$\mathcal{L}_{NEW}^{PV} = \frac{g^2}{4\Lambda^2} \bar{e} \gamma_\mu e \sum_f h_A^q \bar{q} \gamma^\mu \gamma^5 q \quad (17)$$

and  $g$ ,  $\Lambda$  and  $h_A^q$  are, respectively, the coupling constant, the mass scale, and effective coefficients associated with the new physics. The mass limit in our case is therefore

$$\Lambda/g \approx \frac{1}{\sqrt{\sqrt{8}G_F|\Delta(2C_{2u} - C_{2d})|}} \approx 1.0 \text{ TeV}. \quad (18)$$

### 1.6.2 $Z'$ Searches

Neutral gauge structures beyond the photon and the  $Z$  boson have long been considered as one of the best motivated extensions of the SM [30]. They are predicted in most Grand Unified Theories (GUT) and appear in superstring theories. Such a gauge boson is called a  $Z'$ . There may be a multitude of such states at or just below the Planck scale, and there exist many models in which the  $Z'$  is necessarily located at or near the weak scale. Only the light  $Z'$  is of interest here.

Since a  $Z'$  which couples to  $Z^0$  will strongly affect the observables around the  $Z$ -pole, which have been measured to a remarkable precision, we only consider a  $Z'$  which does not mix with  $Z^0$ . Direct searches at FNAL have ruled out any  $Z'$  with  $M_{Z'} < 690$  GeV but a heavier  $Z'$  is possible. Such a  $Z'$  can arise in  $E_6$  [31], a rank-6 group and a possible candidate for the GUT. This  $E_6$  breaks down at the Planck scale and becomes the  $SU(3)_C \times SU(2)_L \times U(1)_Y$  symmetry of the familiar SM. The breaking of  $E_6$  to the SM will lead to extra  $Z$ 's and it is possible that at least one of these is light enough to be observed. The effect of a  $Z'$  in  $E_6$  might be observed in neutrino DIS, PV e-N scattering, PV Møller scattering and APV.

The mass limit on  $Z'$  can be obtained from Eq. (18). From simple models based on GUT one expects  $g \approx 0.45$  [29], giving  $M_{Z'} \approx 0.45$  TeV. Moreover, for  $Z'$  models and also for the SM itself, there is a fortuitous effect, which is that  $2C_{2u} - C_{2d} = 3(2C_{1u} + C_{1d})$ . Thus instead of a  $Z'$  search of 0.45 TeV, one is instead sensitive to a limit higher by  $\sqrt{3}$ , giving about  $M_{Z'} \approx 0.8$  TeV.

### 1.6.3 Compositeness and Leptoquark (LQ)

If quarks and leptons have intrinsic structure (compositeness), then there may be an interchange of fermion constituents at very short distances [1]. The lowest dimension contact interactions are the four-fermion contact interactions between quarks and leptons, described by 8 relevant terms  $\bar{e}_i \gamma_\mu e_i \bar{q}_j \gamma^\mu q_j$  where  $i, j = L, R$  and  $q = u, d$  [34]. They lead to a shift in couplings [35]

$$\Delta C_{1q} = \frac{1}{2\sqrt{2}G_F(\eta_{RL}^{eq} + \eta_{RR}^{eq} - \eta_{LL}^{eq} - \eta_{LR}^{eq})} \quad (19)$$

$$\Delta C_{2q} = \frac{1}{2\sqrt{2}G_F(-\eta_{RL}^{eq} + \eta_{RR}^{eq} - \eta_{LL}^{eq} + \eta_{LR}^{eq})} \quad (20)$$

In theories that predict quark and lepton compositeness, there are new strong confining dynamics at a scale  $\Lambda$ . Any contact terms produced by the strong dynamics will respect its global symmetries, and it is not difficult to find such global symmetry (other than parity) which ensure cancellations in the change in  $C_{1q}$ 's. For instance, an approximate global  $SU(12)$  acting on all left handed first generation quark states will cause no effect on  $C_{1q}$ 's while still allow a non-zero contribution to  $C_{2q}$ 's ( $LL = -LR, RL = -RR$ ) [33]. Therefore, measurement of  $C_{2q}$ 's will

provide a unique opportunity to explore quark and lepton compositeness. Using the formalism of Ref. [32], a four-fermion contact interaction of form  $\pm \frac{4\pi}{\Lambda_1^2} \bar{l}_{\mu L} \gamma^\mu l_{\mu L} \bar{q}_L \gamma^\mu q_L$  will change  $C_{2q}$ 's by  $\pm \frac{\sqrt{2}}{G_F} \frac{\pi}{\Lambda_1^2}$  where  $\Lambda$  gives the scale of the interaction. Thus the measurement on  $C_{2q}$ 's proposed here will set a limit of  $\Lambda_1 > 3.56$  TeV. Although this is somewhat lower than the mass limits given in Ref. [35, 36] where the most recent HERA data [37] are included, the limits there were obtained by allowing one contact term at a time, and setting all others to zero. Ultimately we need information on all parameters simultaneously and results from the proposed measurement will provide important inputs to such a fit.

Leptoquarks are vector or scalar particles carrying both lepton and baryon numbers. For DIS-parity, the presence of LQ will change the observed asymmetry by an amount proportional to  $\lambda^2/4M_{LQ}^2$  where  $M_{LQ}$  is the mass of LQ and  $\lambda$  is its coupling to electron and quarks. Assuming for simplicity creation of a scalar leptoquark from interactions with  $u$  quarks but not  $d$  quarks, one can use Eq. (18) but need to multiple the r.h.s. by factor of  $\sqrt{2}$  for the scalar LQ case. The measurement on  $2C_{2u} - C_{2d}$  proposed here will thus set a limit of

$$\lambda_s \leq 0.14(M_{LQ}/100 \text{ GeV}), \quad (21)$$

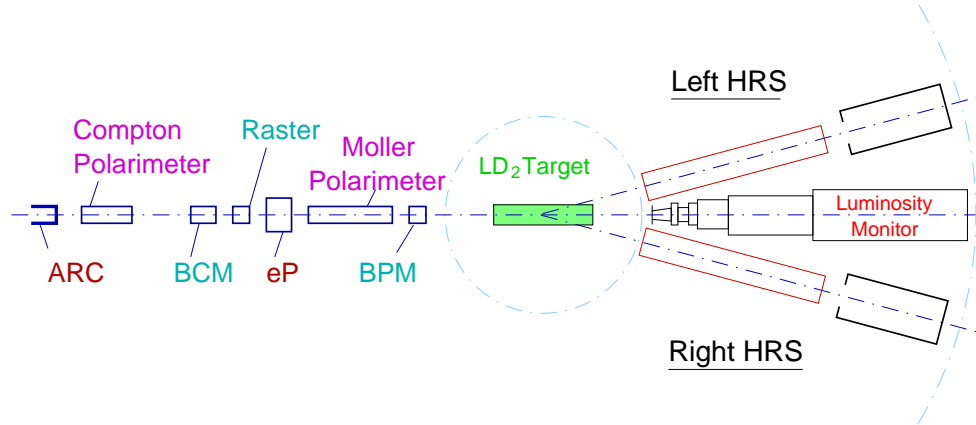
comparable to the current limit from the Cs APV experiment.

## 2 Experimental Setup

### 2.1 Overview

The floor plan for Hall A is shown in Fig 4. We use an  $85 \mu\text{A}$  polarized beam and a 25 cm liquid deuterium target. The scattered electrons are detected by the two standard Hall A High Resolution Spectrometers (HRS). A fast Data Acquisition (DAQ) system will be built to accommodate a rate as high as 1 MHz from each HRS. A Luminosity Monitor (Lumi) is located downstream on the beam-line to monitor the helicity-dependent target boiling effect and possible false asymmetries to a  $10^{-7}$  level. We will describe the instrumentation in the next few sections.

Figure 4: Hall A floor plan for the proposed measurement.



## 2.2 Beam Line

We propose to use 6.0 GeV polarized beam with a 80% polarization and 85  $\mu\text{A}$  beam current. To reduce the heat impact on the target, the beam is circularly rastered such that the beam spot size at the target is  $\approx 4$  mm in diameter. The beam energy can be measured to a  $\Delta E/E = 2 \times 10^{-4}$  level using either ARC or eP devices [39]. We need 1% precision in the beam polarization measurement in order to achieve an acceptable systematic uncertainty on the final results. We plan to upgrade the Hall A Compton polarimeter (see next paragraph) to provide this 1% precision. We will also use additional information from the Møller polarimeter (with an upgrade already proposed by the approved experiment E00-003 [40]) to cross-check the Compton results.

The current systematic uncertainty of the Compton polarimeter is about 1.9% for IR laser, 6 GeV beam and electron detection mode (1.8% from calibration, 0.25% from beam properties and 0.5% from laser polarization). An upgrade to a green laser is already planned [41] and will reduce the uncertainty due to calibrations to 0.9%. If the current 600  $\mu\text{m}$  micro-strips used in the electron detector can be upgraded to 300  $\mu\text{m}$  [41], the uncertainty due to calibrations will be improved further by a factor of two ( $\approx 0.5\%$ ), giving a total systematic uncertainty of 0.75%. The cost estimate for upgrading the electron detector proposed here is  $\approx \$ 30 \text{ K}$ <sup>3</sup> for the parts and  $\approx 5$  calendar days facility development time (beam can be on during the last 2 days).

For the Compton polarimeter one can also use the photon analysis method based on either the response function type (currently being used) or on the integration of the photon signal (currently being tested). The preliminary results from the photon integration are promising and this method is believed to be accurate at the 1% level for 6 GeV beam. Thus it will provide a check of the electron analysis result with independent detector and analysis. The photon integration method will be used in the 2005 running of HAPPEX II. Overall, we will use 1% in the analysis of systematic uncertainties.

Currently the Møller polarimeter in Hall A can provide 3% precision. Upgrades have been proposed by an approved experiment (E03-003, Pb-parity) for the Møller to reach a precision of  $\leq 1\%$  [40]. We will use Møller (if available on time) as a cross check for the Compton polarimeter.

## 2.3 Parity DAQ (Hall A)

The parity DAQ in Hall A [42] and the beam helicity feedback system have been successfully used to control the beam helicity-dependent asymmetry for the Hall A parity experiments in the past. The asymmetry in the integrated beam current measured by the parity DAQ is sent to the polarized electron source where the Pockel cell voltage is adjusted accordingly to minimize the beam intensity asymmetry. The beam helicity asymmetry can be controlled to the  $10^{-7}$  level. The false asymmetry caused by the beam helicity asymmetry should be much smaller than this number (since it is a second order effect). This is sufficient for the proposed measurement.

---

<sup>3</sup>This number only includes the cost of new strip planes, 5 strip planes (4 to use + 1 spare) are needed. The cost of a 600  $\mu\text{m}$  plane is \$2.35K in year 2003. An extra \$16K is needed for a new mask to produce the new 300  $\mu\text{m}$  strip size. Cost for manpower is not included here.

## 2.4 The Liquid Deuterium Target

We plan to use a 25-cm long cryogenic liquid deuterium ( $\text{LD}_2$ ) target at its highest cooling power, limiting the beam current to  $85\text{-}\mu\text{A}$ . The target density is  $0.167\text{ g/cm}^3$ . The end-caps of the cell are made of 3 mil Be. The end-cap contamination will be measured using two empty targets with different end-cap thicknesses.

### 2.4.1 Boiling Effect

The target boiling effect has two meanings. The first one is the “local boiling effect”, which is the real phase change of the liquid target. We require zero local boiling for the proposed measurement. The second meaning is usually used for parity experiments. In this case, “target boiling” is a terminology for (1) the change in target density due to heating of the target, for example, change in density due to deviation in beam parameters, mostly spot size; and (2) pulse-to-pulse target density fluctuation. The latter may cause a false asymmetry and will affect the measurement. We will discuss it in the next subsection. The first one will generate a noise (“boiling noise”) in the signal which is equivalent to an additional statistical fluctuation, as described below.

The rate for the proposed measurement is around  $(150 - 500)\text{ kHz}$  (see section 3.11). The statistical uncertainty per beam pulse pair (33 ms  $\text{H}^+$  and 33 ms  $\text{H}^-$ , hence total is 66 ms) is on the order of  $\pm 0.01$ . If the noise from target boiling effect is controlled at the same level as previous HAPPEX I (200 ppm in 1998) and HAPPEX II (100 ppm in 2004) experiments, then the effect on the statistical width of the measured asymmetry will be negligible. The control of the target boiling noise can be monitored by the luminosity monitor, as will be described in section 2.5.

### 2.4.2 Helicity Dependent Density Fluctuation

The measured parity-violating asymmetry of  $\bar{e}\text{-}^2\text{H}$  scattering is expected to be  $\approx 100\text{ ppm}$ . The helicity dependent density fluctuation should be controlled to under 0.05% of this value, *i.e.*, 0.05 ppm. The Luminosity Monitor in Hall A will monitor this quantity. Taking advantage of the high rate at small angle, it is possible to monitor the false asymmetry to a 100 ppb level within each beam helicity pulse, and hence guarantee the control of the density fluctuation to an acceptable level. The luminosity monitor will be described in the next section. The target cooling system and the boiling effects will be tested during commissioning runs.

## 2.5 Luminosity Monitor

Luminosity Monitors (Lumi) were successfully used for the SAMPLE experiment at MIT-BATES, the A4 experiment at MAINZ [43], the E158 experiment at SLAC [44] and the G0 experiment in Hall C. In Hall A, a luminosity monitor built by the MIT group [45] was used in the 2004 running period of HAPPEX II [46] and will be used by the 2005 run of HAPPEX II and the Pb parity experiment [40]. The main purpose of Lumi is to measure an essentially zero asymmetry during normal running of the experiment, to a very high precision. The main effect that Lumi is supposed to monitor is the target boiling effect. Lumi is also used to monitor all other general false asymmetries (for example, the possible beam energy asymmetry).

The Hall A Lumi consists of 8 pieces of quartz at  $0.5^\circ$ . Each piece has  $2 \times 5\text{ cm}^2$  effective area at 7 m from target. The rate for 6-GeV beam is  $> 10^{11}\text{ Hz}$  per piece [47]. With this high

rate, the false asymmetry and the target boiling effect has been monitored to a level of 100 ppm per pulse during the 2004 running of HAPPEX II for a 70  $\mu\text{A}$  current and a  $5 \times 5$  mm raster. With a 85  $\mu\text{A}$  current and a  $2 \times 2$  mm raster being proposed here, the noise level is expected to be controlled below the  $10^3$  ppm level, thus will add negligible effect to the statistical width of the measured asymmetry (0.01 per pulse).

Most of the events in Lumi are elastic. The asymmetry is in general proportional to  $Q^2$ , hence the physics asymmetry detected by Lumi is very small, of the order of  $< 100$  ppb. Therefore the false asymmetry can be monitored to  $\approx 100$  ppb. This will cause a  $< 0.1\%$  systematic uncertainty to the measured asymmetry which is sufficient for the proposed measurement.

## 2.6 Spectrometers

We use the standard Hall A High Resolution Spectrometer (HRS) to detect the scattered electrons. For each HRS the effective solid angle acceptance for an extended target is 5.4 msr and the momentum bite is  $\pm 4.5\%$ . The central momentum of the HRS can be calculated from the dipole field magnitude and the HRS constant to the  $5 \times 10^{-4}$  level [48]. The HRS central angle can be determined to  $\pm 0.2$  mrad using  $H(e, e'p)$  elastic scattering data, with careful analysis [49].

Partical identification (PID) in each HRS will be done with a  $\text{CO}_2$  Čerenkov detector and a double-layered lead glass shower detector. Based on data from the past experiments, the combined pion rejection factor of the detectors was found to be  $\geq 10^4$  [50], provided that the electron efficiency of each one to be  $\geq 99\%$ . At high rate, a practical estimate of the PID efficiency should also take into account the effect of event pileup, detector readout deadtime and electronic noise. We simulated these effects and find that the pion rejection with the fast counting DAQ should be better than  $10^3$ . We will use this value in the analysis of systematics uncertainties (see section 3.4).

## 2.7 Fast Counting DAQ

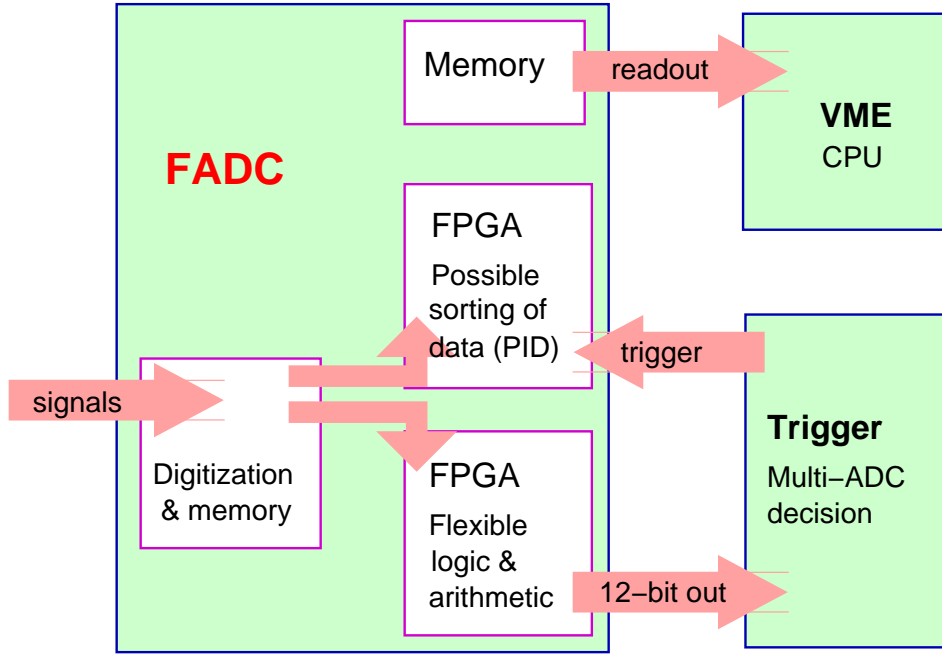
Because of the need to separate the pion background we must use a counting method. The counting method has been used successfully at 100 MHz by the Mainz A4 parity violation experiment [43][51]. Also relevant is the experience of the G0 collaboration in deploying a counting method [52]. Normally an integrating DAQ, in which one integrates the detected flux over the helicity pulse, is preferred for parity violation experiments because it avoids dangerous deadtime corrections. However, we believe we can control this correction as further discussed below.

The detector signals we will use include the ten signals from the gas Čerenkov detector and the approximately 180 signals from two layers of leadglass detectors. In addition, the 24 signals from scintillators might be useful for crude directional information. To process this information we are considering a modified version of the Flash ADC (FADC) which is presently being designed by the Fast Electronics Group at JLab. A schematic diagram is given in Fig. 5. This FADC design will allow for the possibility of counting experiments at approximately 1 MHz with low and precisely measurable deadtime, *e.g.* 1% deadtime measured to 0.3% absolute accuracy. The FADC fills an on-board memory at 250 MHz with  $\approx 4$   $\mu\text{sec}$  latency (buffer size). The information provides both amplitude and timing information about the signal. An on-board processor (FPGA) will analyze the digitized data, with intermediate results sent to an external trigger processor to form a trigger based on on multiple FADC boards. Assuming the processing is fast



Figure 5: Schematic diagram for the fast DAQ system (a possible 2<sup>nd</sup> generation of JLab in-house design).

250 MHz, 2 usec latency, 1 MHz on-board analysis, 0.1% DT measurement



enough there is practically no deadtime in the system, although there will be pileup effects, as discussed below. The scheme will be flexible enough to accommodate a variety of experiments. The FADCs are being built for the Hall A 12 GeV upgrade and this proposal capitalizes on this development. A first version of the FADC should be ready by 2007.

The on-board algorithm shall permit an online identification of electrons, pions, and associated pileups, and counts these in local memory on the FADC. The data which is read out from the FADCs by the VME cpu is the number of counts of these particles integrated over the helicity pulse, usually at 30 Hz, and possibly at a higher sampling rate, say 600 Hz. In a test mode the entire FADC data may be read (at the price of some deadtime) to check the reliability of the algorithm.

Electrons are identified as events which pass above the Čerenkov cut and which deposit a sufficient total energy in the leadglass, while pions leave no signal in the Čerenkov and small average signals in the leadglass. The efficiency of the cuts and the cross contamination of the particle samples can be checked at very low beam current. From experience in Hall A, these efficiencies and contaminations are already known under running conditions similar to the proposal. Pileup of two particles will occur in approximately 6% of events if we make no changes to the existing phototubes which have a 60 nsec resolving time. Although these effects are not

easy to study directly at high rates, we can indirectly study them by an analysis in which the data of independent events are added. The pileup effects include: 1)  $e^- - e^-$ ; 2)  $e^- - \pi$ ; 3)  $\pi - \pi$ . Since electrons must only pass a threshold, electrons accompanied by a secondary particle will still be counted as electrons; however, a correction must be applied for 2 electron pileup. These can be measured using a higher threshold cut on the leadglass and counting the events that pass this higher threshold. At a total rate of 1 MHz (500kHz  $e^-$  and 500kHz  $\pi^-$ ), the pileups involving pions will result in a  $(1.5 - 2.0)\%$  loss of the pion count rate, since they tend to be moved away from the one-pion cut window. A fraction  $(0.5 - 1)\%$  of two pion events will be counted erroneously as electrons. These effects from pions can be corrected with sufficient accuracy and the uncertainty is practically negligible (since the  $\pi/e$  ratio and the pion asymmetry will be measured precisely).

If the processing of the FADC is fast enough we can maintain a deadtime which is very small, probably  $\leq 10$  nsec. However, the system may have a deadtime of order 1% which could be different for different physical processes. Our goal is to measure the deadtime correction to the physics asymmetry with an absolute accuracy  $\pm 0.3\%$ . To ensure reliability it is important to measure the deadtime with at least two independent methods as follows. A first method is to pulse the detector channels with a light sources whose amplitude and pulse shape is similar to those of real particles, and count how many of these signals are subsequently identified by the electronics. A second method is to introduce a deliberate programmed deadtime into the frontend, thus making it predictable and understood.

## 2.8 Data Analysis

### 2.8.1 Extracting Asymmetry $A_d$ from Data

The parity violating asymmetry of  $\vec{e}^- - {}^2\text{H}$  scattering is extracted from the measured raw asymmetry as

$$A_d = \frac{A_{raw}}{P_{beam}} + \Delta A_{EM}^{RC} \quad (22)$$

where  $P_{beam} = (80\% \pm 0.8)\%$  is the beam polarization. We will discuss in more details the electromagnetic radiative correction  $\Delta A_{EM}^{RC}$  in section 3.6.

### 2.8.2 Extracting $2C_{2u} - C_{2d}$ from $A_d$

From Eq. (11), one can extract  $2C_{2u} - C_{2d}$  from the leading twist asymmetry  $A_{d,LT}$  as

$$2C_{2u} - C_{2d} = a_2 A_{d,LT} + b_2 \quad (23)$$

where  $a_2$  and  $b_2$ , if the electroweak radiative corrections are not included, are given by

$$a_2 = \frac{1}{\mathcal{K}Q^2} \frac{5 + R_s + 4R_c}{Y R_v}, \quad (24)$$

$$b_2 = -\frac{2C_{1u}(1 + R_c) - C_{1d}(1 + R_s)}{Y R_v}, \quad (25)$$

with  $\mathcal{K} \equiv \frac{3G_F}{\pi\alpha 2\sqrt{2}} = 539.5 \text{ ppm/GeV}^2$  and  $R_c$ ,  $R_s$  and  $R_v$  are defined by Eq. (13). For  $C_{1q}$  we use the Standard Model values Eq. (1-2) and  $\sin^2 \theta_W = 0.235$ . With electroweak radiative corrections, Eq. (28-29) (see section 3.7) need to be used for  $C_{1q}$ 's in Eq. (25). We used MRST2002 [53] and CTEQ6M [54] PDF fits to evaluate  $R_c$ ,  $R_s$  and  $R_v$  and their uncertainties. The uncertainty in  $2C_{2u} - C_{2d}$  due to the error in PDF fits, kinematic variables, and various other effects will be given in section 3.

### 3 Expected Uncertainties and Rate Estimation

In this section we first estimate the systematic uncertainties for  $A_d$  and theoretical uncertainties for extracting  $(2C_{2u} - C_{2d})$ . Then we give the rate estimate, calculate the statistical uncertainty and in the end give the beam time request for the proposed measurements.

#### 3.1 Deadtime Correction

The uncertainty of the deadtime correction will 0.3% as described in section 2.7.

#### 3.2 Target Purity, Density Fluctuation and Other False Asymmetries

The liquid deuterium usually used contains [55] 1889 ppm HD, < 100 ppm H<sub>2</sub>, 4.4 ppm N<sub>2</sub>, 0.7 ppm O<sub>2</sub>, 1.5 ppm CO (carbon monoxide), < 1 ppm methane and 0.9 ppm CO<sub>2</sub> (carbon dioxide). Compared to the statistical accuracy of the measurement ( $\approx 1.1\%$  in  $A_d$ ), the only non-negligible contamination to the measured asymmetry is from the proton in HD. Since the asymmetry of the proton is given by [22]

$$A_p = \left( \frac{3G_F Q^2}{\pi\alpha 2\sqrt{2}} \right) \frac{2C_{1u}u(x) - C_{1d}[d(x) + s(x)] + Y[2C_{2u}u_v(x) - C_{2d}d_v(x)]}{4u(x) + d(x) + s(x)} \quad (26)$$

which is within  $\pm 10\%$  of the asymmetry of the deuteron, the proton in HD contributes  $\delta A_d/A_d < 0.02\%$  uncertainty to the measured asymmetry. The Luminosity Monitor can make sure that the target density fluctuation is less than 0.1 ppm. This is < 0.1% uncertainty in the measured asymmetry.

#### 3.3 Target End Cap Contamination

The target cell endcaps are made of 7 mil aluminum with 3 mil Be in the central region which the beam goes through. Be has density  $1.848 \text{ g/cm}^3$ , the ratio of yield from endcaps to that from LD<sub>2</sub> is estimated to be  $L_{Be}/L_{LD2} \times \rho_{Be}/\rho_{LD2} = 2.64\%$  for each endcap. This ratio can be measured quickly using an empty target with the same end caps as the LD<sub>2</sub> cell. Since Be has  $Z = 4$ ,  $N = 5$ , the asymmetry of  $\vec{e} - Be$  scattering is not very different from  $A_d$  and can be measured using an empty target with thick Be endcaps. To keep the rate of empty cell runs in each HRS below 500 KHz while minimizing the beam time, we will use an empty cell with 80 times thicker Be endcaps than that of the LD<sub>2</sub> cell for the measurement at  $Q^2 = 1.10 \text{ (GeV/c)}^2$  and the beam time needed is 2.5% of the electron production time. For measurement at  $Q^2 = 1.90 \text{ (GeV/c)}^2$  we will use an empty cell with 100 times thicker endcaps and the beam time is 2.2% of the electron runs. The uncertainty in the extracted asymmetry is  $\approx 0.3\%$ .

### 3.4 Pion Background

#### Pion rate

The rate of pion photo-production was estimated by Wiser's fit [56]. Wiser's fit is expected to be good within a factor of 2. We also used previous DIS data within a very similar kinematic region, and found the real  $\pi^-/e^-$  ratio is very close to half of the value given by Wiser's fit [57]. Nevertheless, we will double the pion rate from Wiser's fit as a conservative estimate for the proposed measurement. The electron rate is calculated using a world fit to  $R$  [58] and the deuteron structure function  $F_2^d$  [59]. The pion to electron ratio is expected to be  $\approx 0.8$  for the low  $Q^2$  and  $\approx 5.3$  for the high  $Q^2$  measurement.

#### PID efficiencies for Hall A detectors

A CO<sub>2</sub> Čerenkov counter and a double-layered lead glass counter will be used for particle identification (PID). The PID efficiencies for the Hall A detectors are well understood. With careful detector calibration and off-line analysis, the combined pion rejection factor was found to be better than  $10^4$  for both spectrometers [50] in the regular counting DAQ mode. With the fast counting mode, signals from the Čerenkov detector, lead glass counters and scintillators are sent to the fast counting system which accumulates the electron and pion events separately. See section 2.7 for the design of fast counting DAQ. Test runs are necessary to check the PID efficiencies with fast counting DAQ. The threshold for the PID units of the DAQ system will be set before the production running based on the test-run results. We expect the combined pion rejection factor with fast counting DAQ to be better than  $\approx 10^3$ .

#### Pion asymmetry

The asymmetry of pion production in the DIS region is expected to be small. We first discuss the possible effect from single spin asymmetries. The single beam-spin azimuthal asymmetry (beam SSA) reported recently by the HERMES collaboration [60] is consistent with zero, but with large uncertainties. The data from JLAB Hall B [61] show an azimuthal beam SSA for  $\pi^+$  electro-production,  $A_{LU}^{\pi^+ \sin \phi} \sim 5\%$ . However, since this is an inclusive measurement that integrates over the out-of-plane angle,  $\phi$ , we do not expect any background from SSA.

The only possible background to the proposed measurement comes from weak interactions between partons. Compared to the measured asymmetry, which comes from the interference term between electromagnetic and weak interactions, this background is suppressed by a factor of 100 – 1000. Since the measured asymmetry is about 100 ppm, the maximum background one can have is less than  $10^{-6}$ , or 0.1% of  $A_d$ .

Experimentally, in the original SLAC experiment [20] the pion asymmetry was found to be smaller than the electron asymmetry. Overall, we expect the pion asymmetry to be well below  $10^{-6}$ . The combined pion rejection factor is expected to be better than  $10^3$ . Hence the asymmetry from the pion background will be less than 0.1 ppm. Compared to the measured electron asymmetry  $\approx 100$  ppm, and considering that the  $\pi/e$  ratio is less than 5 for both kinematics, this is a negligible effect. We will use 0.1% for the  $A_d$  uncertainty due to pion background in the analysis.

Furthermore, the pion asymmetry will be measured using the fast pion counters. And the pion to electron ratio will be determined easily using the regular counting mode DAQ at a lower

beam current and a  $\approx 1$  hour run. One will achieve an uncertainty in the pion asymmetry of

$$\delta A_{\pi^-} = \frac{1}{\sqrt{N_{\pi^-}}} = \frac{1}{\sqrt{\beta \eta_{\pi, det} N_{e^-}}} = \frac{1}{\sqrt{\beta \eta_{\pi, det}}} \delta A_d \approx \frac{1}{\sqrt{\beta \eta_{\pi, det}}} (2\% A_d) \quad (27)$$

where  $\beta$  is the  $\pi^-/e^-$  ratio,  $\eta_{\pi, det}$  is the pion detection efficiency using the fast counting DAQ. To ensure the purity of the pion events, we will use tight PID cuts to select pions hence  $\eta_{\pi} \approx 50\%$ . This gives an uncertainty of  $\delta A_{\pi^-} = 3.3$  ppm for the low  $Q^2$  and  $\delta A_{\pi^-} = 2.1$  ppm for the high  $Q^2$  measurement. Considering the pion rejection factor of  $10^3$ , the effect in  $A_d$  from the pion background will be ensured to be below  $2 \times 10^{-8}$  and  $10^{-8}$  for the low and high  $Q^2$  measurement, respectively.

### 3.5 Pair Production Background

Part of the background of the proposed measurement comes from the pair production  $\gamma \rightarrow e^+e^-$ , where  $\gamma$  is coming from the decay of the electro- and photo-produced  $\pi^0$ 's. The pair production from Bremsstrahlung photons is highly forward-peaked and is not significant for the kinematics proposed here. The estimated positron to electron ratio is  $\alpha \approx 0.087\%$  for  $Q^2 = 1.10$  and  $1.199\%$  for  $1.90$  (GeV/c)<sup>2</sup>. (We used Wiser's fit [56] to calculate the  $\pi^+$  and  $\pi^-$  rates and take the average as the value for  $\pi^0$ , then multiplied by two to give a conservative estimate.) Usually the  $e^+e^-$  pairs are assumed to be symmetric and the asymmetry of the  $e^-$  of the pair production background is the same as the positron asymmetry. Because the pion asymmetry for the proposed measurement is below 1 ppm as discussed in the last section, the asymmetry of positrons (or electrons from  $e^+e^-$  pairs) will be at the same level. Because the  $e^+/e^-$  ratio is below 1%, the effect on  $A_d$  from the pair production background will be well below 0.1 ppm, or 0.1% of  $A_d$ . We will use 0.1% in the uncertainty analysis. We will measure the real positron rate using the regular counting DAQ. The requested beam time for positron runs is 4.0 hours for each  $Q^2$  measurement.

### 3.6 Electromagnetic (EM) Radiative Correction

Figure 3 describes the scattering process at tree level. In reality both the incident and the scattered electrons can emit photons. Consequently when we extract cross sections and asymmetries from the measured values there are electromagnetic radiative corrections to be made. The theory for the EM radiative correction is well developed [62]. The correction can be calculated and the uncertainty in the correction is mainly due to the uncertainty of the structure functions ( $F_2$  and  $R$  for an unpolarized target) that are used in the calculation. The ratio of the radiated (observed) cross section and asymmetry to the un-radiated (Born) ones has been calculated [63] and the uncertainty in the asymmetry correction was found to be at the 0.4% (relative) level, corresponding to an uncertainty of 0.0075 for  $(2C_{2u} - C_{2d})$  at  $Q^2 = 1.10$  and 0.0049 at  $Q^2 = 1.90$  (GeV/c)<sup>2</sup>, respectively.

### 3.7 Electroweak Radiative Correction

The products of weak charges  $C_{1,2u(d)}$  given by Eq. (1-4) are valid only for the case in which there is no electroweak radiative correction. With this correction they are given by

$$C_{1u} = \rho' \left[ -\frac{1}{2} + \frac{4}{3} \kappa' \sin^2(\theta_W) \right] + \lambda_{1u} \quad (28)$$

$$C_{1d} = \rho' \left[ \frac{1}{2} - \frac{2}{3} \kappa' \sin^2(\theta_W) \right] + \lambda_{1d} \quad (29)$$

$$C_{2u} = \rho \left[ -\frac{1}{2} + 2\kappa \sin^2(\theta_W) \right] + \lambda_{2u} \quad (30)$$

$$C_{2d} = \rho \left[ \frac{1}{2} - 2\kappa \sin^2(\theta_W) \right] + \lambda_{1d} \quad (31)$$

The electroweak radiative correction is well determined in the Standard Model, though other Higgs scenarios and/or new physics at the TeV scale will affect the electroweak correction, offering the opportunity for new physics. Standard Model electroweak radiative corrections to  $C_{1,2u(d)}$  have been calculated [64] and are relatively small. The corrections modify the  $\rho$ ,  $\kappa$ , and  $\lambda$  parameters from their tree level values  $\rho = \rho' = \kappa = \kappa' = 1$  and  $\lambda_{1u} = \lambda_{1d} = \lambda_{2u} = \lambda_{2d} = 0$ . A recent evaluation [3, 5] gives  $\rho' = 0.9881$ ,  $\kappa' = 1.0027$ ,  $\rho = 1.0011$ ,  $\kappa = 1.0300$ ,  $\lambda_{1d} = -2\lambda_{1u} = 3.7 \times 10^{-5}$ ,  $\lambda_{2u} = -0.0121$ ,  $\lambda_{2d} = 0.0026$ , changing the asymmetry by  $-2.2\%$  at  $Q^2 = 1.10$  and  $-2.6\%$  at  $Q^2 = 1.90$  (GeV/c)<sup>2</sup>. The error in the SM prediction is dominated by our knowledge of the  $\sin^2 \theta_W$  at the proposed energies, which in turn is dominated by the Z-pole value. This uncertainty (about  $1.6 \times 10^{-4}$  from Z-pole asymmetries or  $1.5 \times 10^{-4}$  from the global fit [5]) would introduce a  $< 0.3\%$  error in the asymmetry. The top quark and Higgs boson masses adjust themselves (at least in the SM) to reproduce the measured value of the mixing angle. The uncertainty from  $\alpha(Q^2)$  is at the  $10^{-4}$  level. The running of  $\sin^2 \theta_W$  can be calculated in perturbation theory because the proposed  $Q^2$  is above hadronic scale and the uncertainty is negligible. Overall, the uncertainty on the corrected asymmetry is less than  $0.2\%$ , corresponding to an uncertainty of  $0.0037$  for  $(2C_{2u} - C_{2d})$  at  $Q^2 = 1.10$  and  $0.0024$  at  $Q^2 = 1.90$  (GeV/c)<sup>2</sup>, respectively.

### 3.8 Experimental Uncertainties ( $Q^2$ and the acceptance)

The largest systematic uncertainty related to the asymmetry is the  $1\%$  uncertainty in the beam polarization. Other sources that will contribute when extracting  $(2C_{2u} - C_{2d})$  from  $A_d$  include that from the uncertainty in beam energy  $\Delta E/E = 2 \times 10^{-4}$  [39], the spectrometer central momentum  $\Delta E'/E' = 5 \times 10^{-4}$  [48], and the scattering angle  $\Delta\theta = 0.2$  mrad [49]. The  $Q^2$  for each kinematic setting will be determined using low beam current and regular counting mode DAQ. The uncertainty in  $Q^2$  is thus given by the uncertainties in  $E$ ,  $E'$  and  $\theta$ . It contributes a  $\Delta(2C_{2u} - C_{2d}) = 0.0039$  and  $0.0019$  uncertainty to the low and high  $Q^2$  point, respectively. From experience of previous polarized experiments in Hall A [65], the acceptance of the HRS can be well simulated and the helicity-dependence of the acceptance is negligible.

### 3.9 Parton Distribution Functions and Ratio $R$

The uncertainty in  $R$  is estimated using a world fit [58]. The uncertainty in  $(2C_{2u} - C_{2d})$  due to  $R$  is about  $0.0013$  for both  $Q^2$  measurements. We used two PDF sets MRST2002 [53] and

CTEQ6M [54] to calculate the quark distribution ratios  $R_c$ ,  $R_s$  and  $R_v$  and the asymmetry  $A_d$ . The uncertainties of each PDF set as well as the difference between two sets are used to estimate the uncertainty in the extracted  $(2C_{2u} - C_{2d})$ . The effects are found to be  $\Delta(2C_{2u} - C_{2d}) = 0.0021$  and  $0.0025$  uncertainty to the low and high  $Q^2$  point, respectively.

### 3.10 Charge Symmetry Violation (CSV)

Charge symmetry implies the equivalence between  $u(d)$  quark distributions in the proton and  $d(u)$  quarks in the neutron. Most low energy tests of charge symmetry find it is good to at least 1% level [66] so it is usually assumed to be justified in discussions of strong interactions. However, charge symmetry is not strictly true since the constituent mass of the  $d$  quark is heavier than the  $u$  quark.

The charge symmetry violating (CSV) distributions are defined as [67]

$$\delta u(x) = u^p(x) - d^n(x), \quad (32)$$

$$\delta d(x) = d^p(x) - u^n(x), \quad (33)$$

where the superscripts  $p$  and  $n$  refer to the proton and neutron, respectively. Eq. (32) is usually referred to as the “majority” CSV term and Eq. (33) is the “minority” CSV term. The relations for CSV in anti-quark distributions are analogous. Taking into account the CSV effect, Eq. (11) becomes

$$A_d = \left( \frac{3G_F Q^2}{\pi \alpha 2\sqrt{2}} \right) \times \frac{2C_{1u}[1 + R_c(x) - R_{\delta d}] - C_{1d}[1 + R_s(x) - R_{\delta u} - R_{\delta s}] + Y(2C_{2u} - C_{2d})[R_v(x) - \frac{R_{\delta u_v}}{3} - \frac{2R_{\delta d_v}}{3}]}{5 + R_s(x) + 4R_c(x) - R_{\delta u} - 4R_{\delta d} - R_{\delta s}} \quad (34)$$

where  $R_{\delta q}$  and  $R_{\delta q_v}$  are defined as

$$\begin{aligned} R_{\delta u} &= \frac{\delta u(x) + \delta \bar{u}(x)}{u(x) + \bar{u}(x) + d(x) + \bar{d}(x)}, \\ R_{\delta d} &= \frac{\delta d(x) + \delta \bar{d}(x)}{u(x) + \bar{u}(x) + d(x) + \bar{d}(x)}, \\ R_{\delta u_v} &= \frac{\delta u_v(x)}{u(x) + \bar{u}(x) + d(x) + \bar{d}(x)} \\ \text{and } R_{\delta d_v} &= \frac{\delta d_v(x)}{u(x) + \bar{u}(x) + d(x) + \bar{d}(x)}. \end{aligned} \quad (35)$$

CSV distributions for the valence quarks can be calculated using phenomenological parton distributions based on [68]

$$\begin{aligned} \delta d_v(x) &= -\frac{\delta M}{M} \frac{d}{dx} [x d_v(x)] - \frac{\delta m}{M} \frac{d}{dx} d_v(x) \\ \delta u_v(x) &= \frac{\delta M}{M} \left( -\frac{d}{dx} [x u_v(x)] + \frac{d}{dx} u_v(x) \right) \end{aligned} \quad (36)$$

where  $\delta M = M_n - M_p = 1.3$  MeV is the mass difference between the neutron and proton,  $\delta m = m_d - m_u = 4.3$  MeV is the mass difference between the *down* and *up* quarks (value taken from Ref.[68]) and  $M$  is the average nucleon mass.

We first used Eq. (36) to calculate the CSV for valence quarks. The valence quark PDF are from MRST2001 [53] and CTEQ6M [54]. For the sea quarks we used a meson cloud MIT-bag model [68]. We find the CSV effect  $\delta q/q$  is  $< 1\%$  for  $u_v$ ,  $s$  and  $\bar{d}$ ,  $(1 - 3)\%$  for  $d_v$  and  $\bar{u}$  and  $(2 - 4)\%$  for  $\bar{s}$ , respectively.

We also studied a recent parameterizations (MRST2003 with theoretical uncertainties) [24] which gave fits for the CSV term in both the valence and the sea quarks. While at the proposed kinematics the new MRST fits give smaller CSV for the valence quarks than Eq. (36), they give an 8% CSV for sea quarks, much larger than the MIT-bag model prediction. Here we take the maximum of the MRST fit and the value from Eq. (36) as an estimate for the valence quark CSV, and take the average of the MRST fit and the MIT-bag model prediction for the sea quark CSV. Overall, the uncertainty from CSV is  $\Delta(2C_{2u} - C_{2d}) = 0.0074$  and  $0.0068$  at the low and high  $Q^2$  point, respectively.

### 3.11 Rate Estimation and Kinematics Optimization

We used the NMC95 unpolarized DIS fit [59] to calculate the  $e^-$  rate. Pion and positron (pair production) backgrounds are estimated using Wiser's [56] fit (with  $\pi^-$  rate multiplied by 2 based on previous data). The optimized kinematics is given in Table 2.

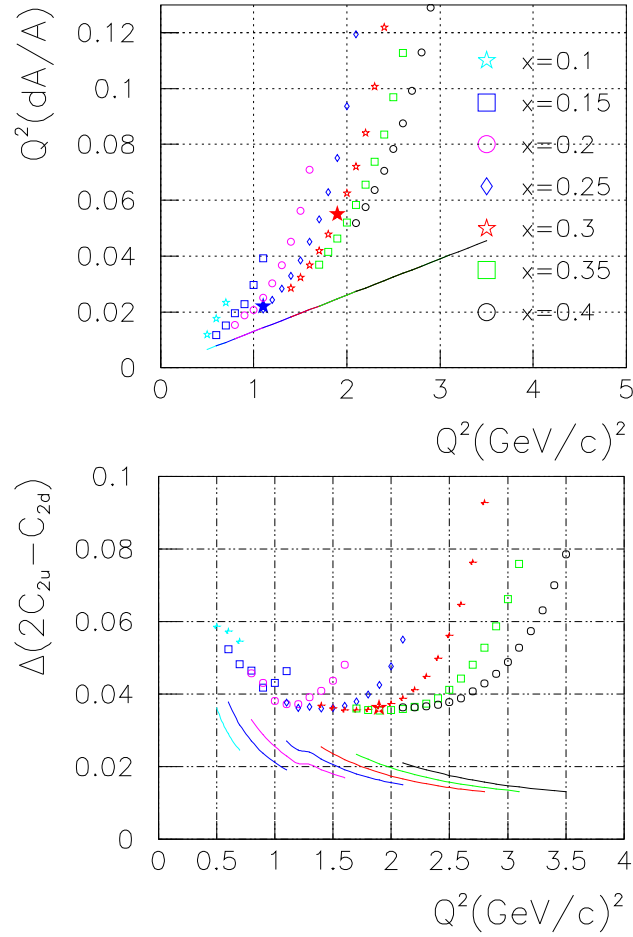
Table 2: Kinematics for the Proposed Measurements. Rates are for **each** HRS and  $\pi^-/e^-$  ratios are two times results from Wiser's fit. The low  $Q^2$  measurement will take place on the left HRS and the high  $Q^2$  measurement will be shared by the two HRSs.

Kinematics	I	II
$x_{Bj}$	0.25	0.30
$Q^2$ (GeV/c) <sup>2</sup>	1.10	1.90
$E$ (GeV)	6.0	6.0
$E'$ (GeV)	3.66	2.63
$\theta$	12.9°	20.0°
$W^2$ (GeV) <sup>2</sup>	4.18	5.31
$Y$	0.471	0.717
$R_c$	$< 0.001$	0.001
$R_s$	0.046	0.044
$R_v$	0.875	0.909
$A_d$ (measured, ppm)	-90.5	-160.6
$e^-$ rate (KHz)	284.6	26.7
$\pi^-/e^-$ ratio	0.8	5.3
$e^+/e^-$ ratio	0.087%	1.199%
total rate (KHz)	501.6	168.1
$e^-$ production time (days)	9.0	32.0
endcap runs	0.2	0.7
$e^+$ runs	0.2	0.2



The optimization of these two kinematics can be seen from Fig. 6, where the uncertainty on the measured asymmetry (left) and on  $2C_{2u} - C_{2d}$  (right) are shown as functions of  $Q^2$ , for kinematics allowed by the HRS and 20 days of beam time. Since the lower  $Q^2$  measurement is to constrain the HT effects for the higher  $Q^2$  point, we choose the two kinematics to have as close  $x$  and as different  $Q^2$  as possible, while minimizing the uncertainty on  $2C_{2u} - C_{2d}$  for the higher  $Q^2$  point. Thus we did not consider kinematics below  $x = 0.2$  although the uncertainty on the asymmetry is expected to be smaller.

Figure 6: Figure of merit for the proposed measurement for kinematics allowed by the HRS and 20 days of beam time. The uncertainties on the measured asymmetry  $\Delta A_d/A_d$  are scaled by  $Q^2$  on the top panel to show the sensitivity to the higher-twist effect. The uncertainties on  $2C_{2u} - C_{2d}$  are shown on the bottom panel, with the systematic uncertainties shown by the colored curves below markers. The chosen kinematics for the lower  $Q^2$  measurement are shown as the blue filled star on the top panel and for the higher  $Q^2$  measurement are shown as the red star on both panels.



### 3.12 Error Budget

Table 3: Expected uncertainties on the asymmetry  $A_d$ . The systematic uncertainties are the same for both  $Q^2$  points.

Source/ $\frac{\Delta A_d}{A_d}$	$Q^2 = 1.10 \text{ (GeV/c)}^2$	$Q^2 = 1.90 \text{ (GeV/c)}^2$
$\Delta P_{beam}/P_{beam} = 1\%$	1%	1%
Deadtime correction	$\approx 0.3\%$	$\approx 0.3\%$
Target endcap contamination	0.3%	0.3%
Target purity	$< 0.02\%$	$< 0.02\%$
Pion background	$< 0.2\%$	$< 0.2\%$
Pair production background	$< 0.2\%$	$< 0.2\%$
systematics	1.30%	1.30%
statistical	2.08%	2.02%
stat.+syst.	2.45%	2.41%

Table 4: Expected uncertainty on  $2C_{2u} - C_{2d}$ .

Source/ $\Delta(2C_{2u} - C_{2d})$	$Q^2 = 1.10 \text{ (GeV/c)}^2$	$Q^2 = 1.90 \text{ (GeV/c)}^2$
Statistical	0.0388	0.0246
Systematics (from $A_d$ )	0.0243	0.0158
Experimental ( $Q^2$ )	0.0039	0.0019
$\Delta R \equiv \sigma_L/\sigma_T$	0.0013	0.0017
Parton Distributions	0.0021	0.0025
Charge Symmetry Violation	0.0074	0.0068
Electro-magnetic Radiative Correction	0.0075	0.0049
Electro-weak Radiative Correction	0.0037	0.0024
total uncertainty	0.0473	0.0307

## 4 Beam Time Request

### 4.1 Beam Time Request

We request 46 days of beam time for a measurement of  $\Delta(2C_{2u} - C_{2d}) = 0.03$ . Within these 46 days, 42.3 days are for production running, including 41.0 for  $e^-$  runs, 8.0 hours for  $e^+$  runs and 0.9 days for measuring the asymmetry of target Be end-caps. We need four days commissioning for commissioning of the fast counting DAQ system and the Compton polarimeter, and measuring  $Q^2$  and checking PID performance with the regular counting DAQ as well as the fast counting DAQ. Table 5 summarizes the details of the proposed measurements. Beam times are

given in “two-HRS equivalent”. For example, electron production data for  $Q^2 = 1.10 \text{ (GeV/c)}^2$  will be collected on the HRS-L within  $2 \times 9.0 = 18$  days, meanwhile the HRS-R is used to collect data for  $Q^2 = 1.90 \text{ (GeV/c)}^2$ . Then both HRS will be collecting data for  $Q^2 = 1.90 \text{ (GeV/c)}^2$  simultaneously for 23 days.

Table 5: Kinematics and estimated running time given in “two-HRS equivalent” (see text for details). Beam time needed for commissioning (four days) is not listed here.

$E_b$ (GeV)	$\theta$	$E_p$ (GeV)	$Q^2$ (GeV/c) <sup>2</sup>	$e^-$ production (days)	$e^+$ run (days)	dummy (days)	total beam time (days)
6.0	12.9°	3.66	1.10	9.0	0.2	0.2	9.4
6.0	20.0°	2.63	1.90	32.0	0.2	0.7	32.9

## 4.2 Beam Time Allocation for Running in Two Phases

Because there will be two major instruments – the Compton polarimeter and the fast counting DAQ – to be upgraded/built and tested for the proposed experiment, it is more realistic to split the run into two phases. We suggest a possible beam time allocation below:

- Phase I: 13 days
  1. 9 days of production running with the HRS-L taking data at  $Q^2 = 1.10 \text{ (GeV/c)}^2$  and the HRS-R at  $Q^2 = 1.90 \text{ (GeV/c)}^2$ , including 0.2 days of  $e^+$  and dummy runs for each.
  2. 4 days of commissioning and systematic checks including commissioning of the fast counting DAQ system and the Compton polarimeter; measuring  $Q^2$  and checking PID performance with the regular counting DAQ as well as the fast counting DAQ.
- Phase 2: 33 days
  1. 9 days of production running with the HRS-L taking data at  $Q^2 = 1.10 \text{ (GeV/c)}^2$  and the HRS-R at  $Q^2 = 1.90 \text{ (GeV/c)}^2$ . This will complete the low  $Q^2$  measurement;
  2. 24 days of production running with both HRS taking data at  $Q^2 = 1.90 \text{ (GeV/c)}^2$ . This will complete the high  $Q^2$  measurement.

The advantage of running the experiment in two phases is several folds: Firstly, the expected uncertainty on the HT and  $C_{2q}$  from the first phase running are  $3.5\%/Q^2$  and  $\Delta(2C_{2u} - C_{2d}) = \pm 0.05$ , respectively. The latter corresponds to a factor of five improvement. These results are already significant. Secondly, depending on the results of the first running, we will have flexibility of beam time allocation for the 2nd phase. This can minimize impacts of possible instrumental problems on the final results.

### 4.3 Overview of Instrumentation and Cost Estimate

Table 6: An overview of instrumentation and cost estimate for the proposed measurement.

Experimental Hall	Hall A
Beam polarimeter	Compton electron detector upgrade ( <i>\$30 K</i> ); Compton photon integration method (under development) as a cross-check of the electron method; Møller upgrade planned for Pb-parity ( <i>estimated 2 years</i> )
Beam line	standard ARC and eP
Beam Helicity Control	Parity DAQ and helicity feedback - well developed
Luminosity Monitor	Well developed, used for HAPPEX II, will be used for Pb-parity
Cryogenic Target	25-cm long LD2 target, maximum Hall A target cooling power needed;
Spectrometers	Two HRS taking data simultaneously
DAQ	A modified FADC system ( <i>currently being designed by the electronics group as part of the 12 GeV upgrade, expect to be ready in 2007</i> )
PID	A gas Čerenkov counter and a double-layered Pb glass shower counter. Pion rej. $> 10^4$ with regular DAQ and $> 10^3$ with fast counting DAQ
Total Cost Estimate	<i>\$30 K</i>

## 5 Summary

We propose to measure the parity violating asymmetry  $A_d$  for  $\vec{e}-^2\text{H}$  deep inelastic scattering at  $Q^2 = 1.10$  and  $1.90 \text{ (GeV/c)}^2$  and similar  $x$  using a 25-cm liquid deuterium target in Hall A and  $85 - \mu\text{A}$  polarized beam. Assuming an 80% beam polarization, we request 46 days of beam time to reach an uncertainty on the effective coupling constant  $\Delta(2C_{2u} - C_{2d}) = \pm 0.03$ . The running of the experiment is divided into two phases: phase I of 13 days and phase II of 33 days.

The proposed measurement is the first step of the DIS-parity program at JLab. The expected precision on  $2C_{2u} - C_{2d}$  will improve the current knowledge on this quantity by a factor of eight. The result will help to extract  $C_{3q}$  from high energy data, and has the potential to reveal possible new physics beyond the Standard Model. The higher-twist effects explored by the low  $Q^2$  measurement will provide the first, crucial guidance on the interpretation of existing data and on the future DIS-parity measurements for the JLab 12 GeV upgrade.

## Acknowledgment

We would like to thank Stanley Brodsky, Wally Melnitchouk, Piet Mulders, Willy van Neerven and Fabian Zomer for useful discussions and David Lhuillier for helping with technical issues.

## References

- [1] M.J. Ramsey-Musolf, Phys. Rev. **C60**, 015501 (1999).
- [2] J. Erler and M.J. Ramsey-Musolf, arXiv: hep-ph/0404291.
- [3] *Particle Data Group*, Phys. Rev. D **66**, 010001 (2002); <http://pdg.lbl.gov>.
- [4] E.J. Beise, M.L. Pitt and D.T. Spayde, Prog. Part Nucl. Phys. **54**, 289 (2005) (available on [www.sciencedirect.com](http://www.sciencedirect.com)).
- [5] *Review of Particle Physics*, S. Eidelman *et al.* Phys. Lett. B **592**, 1 (2004); <http://pdg.lbl.gov>.
- [6] A. Argento *et al.* Phys. Lett. B **120**, 245 (1983).
- [7] A. Czarnecki and W.J. Marciano, arXiv: hep-ph/0003049.
- [8] J. Erler, Contribution to the Fermilab Workshop on "QCD and Weak Boson Physics" at the Tevatron Run II; arXiv: hep-ph/0005084.
- [9] A.I. Milstein, O.P. Sushkov, I.S. Terekhov, hep-ph/0212072 (2002); Phys. Rev. Lett. **89**, 283003 (2002); V.A. Dzuba, V.V. Flambaum, J.S.M. Ginges, Phys. Rev. **D66**, 076013 (2002).
- [10] G.P. Zeller *et al.* (NuTeV Collaboration), Phys. Rev. Lett. **88**, 091802 (2002).
- [11] M. Chanowitz, Phys. Rev. Lett. **87**, 231802 (2001); Phys. Rev. **D66**, 073002 (2002).
- [12] R. Carlini *et al.* ( $Q_{\text{weak}}$  Collaboration) "The  $Q_{\text{weak}}$  Experiment: A Search for New Physics at the TeV Scale Via a Measurement of the Proton's Weak Charge", (2001).
- [13] K.S. Kumar *et al.*, (SLAC E-158-Møller Collaboration) "A Precision Measurement of the Weak Mixing Angle in Møller Scattering", SLAC Proposal E-158.
- [14] P.C. Rowson, D. Su and S. Willocq, Highlights of the SLD physics program at SLAC, Ann. Rev. Nucl. Part. Sci., **51**, 345 (2001).
- [15] A Combination of Preliminary Electroweak Measurements and Constraints on the Standard Model. Technical Report CERN-EP/2001-98, (2001), arXiv: hep-ex/0112021.
- [16] G.W. Bennett *et al.* (Muon g-2 Collaboration), Phys. Rev. Lett. **92**, 161802 (2004); G.W. Bennett *et al.* (Muon g-2 Collaboration), Phys. Rev. Lett. **89**, 101804 (2002); H.N. Brown *et al.* (Muon g-2 Collaboration), Phys. Rev. Lett. **86**, 2227 (2001).

- [17] C.S. Wood *et al.*, Science, **275**, 1759 (1997); S.C. Bennet and C .E. Wieman, Phys. Rev. Lett. **82**, 2484 (1999);
- [18] J.T. Londergan, A.W. Thomas, Phys. Lett. B **558**, 132 (2003).
- [19] Preliminary results of E158 Run I-III, see <http://www.slac.stanford.edu/exp/e158/plots/results.html>
- [20] C.Y. Prescott, *et al.*, Phys. Lett. B **77**,347 (1978).
- [21] R.N. Cahn and F.J. Gilman, Phys. Rev. D **17**, 1313 (1978).
- [22] P.E. Bosted *et al.* (SLAC E-149 Collaboration), “DIS-Parity: Parity Violation in Deep Inelastic Electron Scattering”, SLAC Proposal E-149 (1993).
- [23] M. Virchaux and A. Milsztajn, Phys. Lett. B **274**, 221 (1992).
- [24] A.D. Martin, R.G. Roberts, W.J. Stirling and R.S. Thorne, Eur. Phys. J. C **35**, 325 (2004).
- [25] P. Castorina and P.J. Mulders, Phys. Rev. D **31**, 2760 (1985).
- [26] S. Fajfer and R. J. Oakes, Phys. Rev. D **30**, 1585 (1984).
- [27] W.L. van Neerven, *priv. comm.*; X. Zheng *et al.*, JLab LOI 03-106, June 2003.
- [28] M. Gluck and E. Reya, Phys. Rev. Lett. **47**,1104 (1981).
- [29] J. Erler, A. Kurylov and M.J. Ramsey-Musolf, Phys. Rev. D **68**, 016006 (2003).
- [30] Section by K.S. Babu and C. Kolda, *The Z' Searches*, in K. Hagiwara *et al.* (Particle Data Group), Phys. Rev. D **66**, 010001 (2002); <http://pdg.lbl.gov>.
- [31] D. London and J.L. Rosner, Phys. Rev. D **24**, 1530 (1986).
- [32] P. Langacker, M. Luo and A.K. Mann, Rev. Mod. Phys. **64**, 87 (1992).
- [33] A.E. Nelson, Phys. Rev. Lett. **78**, 4159 (1997).
- [34] E. Eichten, K.D. Lane, M.E. Peskin, Phys. Rev. Lett. **50**, 811 (1983).
- [35] D. Zeppenfeld and K. Cheung, arXiv: hep-ph/9810277.
- [36] K. Cheung, Phys. Lett. B **517**, 167 (2001).
- [37] C. Adloff *et al.*, (H1 Collaboration), Z. Phys. C, **74**, 191 (1997); J. Breitweg *et al.* (ZEUS Collaboration), Z. Phys. C **74**, 207 (1997).
- [38] E. Leader and E. Predazzi, *An Introduction to Gauge Theories and Modern Particle Physics*, Vol. 2, Cambridge University Press (1996).
- [39] J. Alcorn *et al.*, Nucl. Instrum. Meth. A **522**, 294 (2004).

- [40] R. Michaels *et al.*, Neutron skin of  $^{208}\text{Pb}$  Through Parity Violating Electron Scattering, An update of E00-003, PAC 23 proposal, accepted, A rating.  
<http://www.jlab.org/rom/pbupdate.ps>
- [41] D. Lhuillier, *priv. comm.*
- [42] B. Humensky, *General exam advanced project*, Princeton University (1999); B. Humensky, *Ph.D. Thesis*, Princeton University (2003).
- [43] D. von Harrach, F.E. Maas *et al.*; <http://www.kph.uni-mainz.de/A4/>
- [44] G.M. Jones, *Luminosity Monitor*, E158 Technical Note, updated 9/11/01 (2001).
- [45] R. Suleiman, *A Conceptual Design of Hall A Luminosity Monitor*, presentation on Hall A parity collaboration meeting, September 2002.
- [46] K. Kumar and D. Lhuillier, JLAB experiment E99-115,  
[http://www.jlab.org/exp\\_prog/CEBAF\\_EXP/E99115.html](http://www.jlab.org/exp_prog/CEBAF_EXP/E99115.html).
- [47] R. Suleiman, *priv. comm.*
- [48] N. Liyanage, *Spectrometer constant determination for the Hall-A High Resolution Spectrometer Pair*, Jefferson Lab Hall A technote, JLAB-TN-01-049.
- [49] H. Ibrahim, P. Ulmer, N. Liyanage, JLAB Hall A Technical Notes JLAB-TN-02-032, (2002).
- [50] X. Zheng, *JLAB Hall A detector PID efficiency analysis using high electron and high pion rate data*, see E99-117 website <http://hallaweb.jlab.org/physics/experiments/he3/A1n/>
- [51] S. Koebis, P. Achenbach, *et.al.*, Nucl. Phys. B (Proc. Suppl.) **61B**, 625 (1998).
- [52] G. Batigne, *et.al.*, “Deadtime Corrections for the French Electronics”, G0 Internal Memo.
- [53] A.D. Martin, R.G. Roberts, W.J. Stirling and R.S. Thorne, arXiv: hep-ph/0211080.
- [54] CTEQ: The Coordinated Theoretical-Experimental Project on QCD; J. Pumplin, D.R. Stump, J. Huston *et al.*, J. High Energy Phys. **07**, 012 (2002).
- [55] M. Seely, *Gas Chromatograph Analysis for Deuterium Sample*, July 26, 2002.
- [56] D.E. Wiser, *Ph.D. thesis*, Univ. of Wisconsin, (1977);
- [57] Here is a comparison of Wiser’s fit to data. Data are from E97-103 in Hall A using a  $^3\text{He}$  target (K. Kramer *priv. comm.*), the calculated  $\pi^-/e^-$  ratio has taken into account the pion decay.

$E_b$	$\theta$	$E'$	$\pi^-/e^-$ (data)	$\pi^-/e^-$ (Wiser)
3.46579	18.592	1.600	1.635	3.430
4.59825	18.592	1.990	2.255	4.051
4.59825	15.798	2.290	1.010	1.897
5.7269	15.798	2.630	1.459	2.506
5.7269	18.585	2.270	3.252	5.258

- [58] K. Abe *et al.*, Phys. Lett. B **452**, 194 (1999).
- [59] M. Arneodo *et al.*, Phys. Lett. B **364**, 107 (1995).
- [60] A. Airapetyan *et al.*, Phys. Rev. Lett. **84**, 4047 (2000).
- [61] H. Avakian *et al.*, Phys. Rev. D **69**, 112004, (2004).
- [62] L. Mo, Y.S. Tsai, Rev. Mod. Phys. **41**, 205 (1969).
- [63] R. Arnold, P.E. Bosted, S.E. Rock *et al.*, *DIS-parity – Search for New Physics Through Parity Violation in Deep Inelastic Electron Scattering*, SLAC-LOI-2003-1 (2003)
- [64] W.J. Marciano and A. Sirlin, Phys. Rev. D **29**, 75 (1984).
- [65] X. Zheng, Ph.D. Thesis, Massachusetts Institute of Technology, (2002).
- [66] G.A. Miller, B.M.K. Nefkens and I. Salus, Phys. Rep. **194**, 1 (1990).
- [67] J.T. Londergan, A.W. Thomas, Phys. Lett. B **558**, 132 (2003); C. Boros, J.T. Londergan and A.W. Thomas, Phys. Rev. Lett, **81**, 4075 (1998).
- [68] E. Sather, Phys. Lett. B **274**, 433 (1992).